

Hyper-Rayleigh light-scattering spectra determined by *ab initio* collisional hyperpolarizabilities of He-Ne atomic pairs

W. Głaz,¹ T. Bancewicz,^{1,*} J.-L. Godet,² G. Maroulis,^{3,†} and A. Haskopoulos³

¹*Nonlinear Optics Division, Faculty of Physics, Adam Mickiewicz University, 61-614 Poznań, Poland*

²*Laboratoire des Propriétés Optiques des Matériaux et Applications, Université d'Angers, 2 boulevard Lavoisier, 49045 Angers, France*

³*Department of Chemistry, University of Patras, GR-26500 Patras, Greece*

(Received 5 January 2006; published 17 April 2006)

The collision-induced (CI) first hyperpolarizability tensor for the He-Ne pair composed of the lightest noble gas elements has been obtained on the grounds of an *ab initio* method as a function of the interatomic distance R . Collision-induced hyper-Rayleigh (CIHR) spectra scattered in mixtures of such atoms at temperatures of 95 and 295 K are computed in absolute units both quantum mechanically and classically for the frequency shifts up to 1000 cm^{-1} . The spectral features of the CIHR profiles due to the vector b_1 and septor b_3 parts of the hyperpolarizability tensor are discussed. The quantum character of computed spectra, especially significant at lower temperatures, has been found out. The integrated intensities of the spectra have been evaluated and used as a criterion of the reliability of the computed profiles. The frequency-dependent depolarization ratio of the CIHR spectra was evaluated and discussed. The properties of the resulting HR profiles have been compared with the depolarized CI Rayleigh spectrum of the He-Ne pair.

DOI: [10.1103/PhysRevA.73.042708](https://doi.org/10.1103/PhysRevA.73.042708)

PACS number(s): 33.80.Gj, 34.30.+h

I. INTRODUCTION

When a molecular microsystem is immersed in the electric field of a light beam of a high photon density, there is, by no means, a non-negligible probability of the occurrence of three-photon scattering: the molecule “absorbs” simultaneously two photons (of circular laser frequency ω_L) and “emits” a photon of the doubled frequency $2\omega_L$ in a process of spontaneous three-photon scattering referred to as hyper-Rayleigh (HR) scattering. The earliest research into nonlinear three-photon light scattering from molecular liquids is due to the experimental works by Terhune, Maker, and Savage [1] and a compact classical and quantum theory of multipolar harmonic scattering proposed by Kielich [2,3]. Those theoretical predictions based on the second-order quantum electrodynamic perturbative treatment led to the conclusion that HR intensity is described by the hyperpolarizability tensor b_{ijk} [1–7].

For many years the HR scattered intensities have been attributed to the first hyperpolarizability tensor \mathbf{b} of individual molecules [8–13]. However, quite analogously as in the case of linear optics [14–16], interactions between monomers of a system may to some extent contribute to the HR signal [17–19]. For centrosymmetric scattering microsystems the first hyperpolarizability tensor b_{ijk} vanishes identically therefore no HR signal is expected. Intermolecular interactions, however, often break the symmetry [20] and the process, forbidden in a monomer description, is observed already at the level of the binary regime (i.e., for dissimilar atomic pairs). This mechanism may well apply to a binary mixture of unlike atoms considered by us.

In recent years the theoretical analysis of collision-induced spectroscopic observation (CISO) can pave the way to the rationalization of related phenomena, bringing forth new insights and fundamental knowledge [20–25]. The theory of electric multipole moments and electric multi- and hyperpolarizabilities [26] has emerged as a key ingredient of the theoretical analysis of such observations. It has been clearly shown that the CISO can also yield estimates of, otherwise not easy amenable to experiment, properties of the interacting systems [27–31]. Thus high-level computational chemistry can make a substantial contribution to the above efforts by predicting accurate properties for the interacting monomers. In more recent works, it has been shown that the determination of the hyper-Rayleigh scattering intensities in simple systems such as the rare-gas heterodiatoms Ne-Ar (Refs. [32,33]) and Kr-Xe (Refs. [34,35]) leans heavily on the knowledge of the interaction (hyper)polarizability for a wide range of intermolecular separations. The calculation of these interaction properties is based on a computational philosophy presented in detail in a previous work [36].

Recently, we have published results of quantum-mechanical and classical CIHR computations for the relatively heavy Ne-Ar [32] and Kr-Xe [34] supermolecules. In this paper, we present a theory and numerical calculations of the CI hyper-Rayleigh spectrum of the He-Ne mixtures, consisting—on the contrary—of the least massive noble gas atoms. Theoretical studies of this kind are of growing importance at the dawn of the era of extremely precise spectroscopic experiments, allowing measurements of such subtle collisional effects.

The details of the theory, both quantum mechanical and classical, have been given in Sec. II. Section III contains numerical considerations: the datasets used for the collisional molecular properties as well as the details of the numerical calculations applied. In this section the *ab initio* computations of the CI hyperpolarizability tensor \mathbf{b} for He-Ne are

*Corresponding author.

Email address: tbancewi@zon12.physd.amu.edu.pl

†Corresponding author. Email address: maroulis@upatras.gr

described; the distance dependence of this tensor is also emphasized. Moreover, in Sec. III numerical procedures, either quantal and classical, concerning both the CIHR spectra and their zeroth moments, are presented; with the quantities expressed in absolute units. The frequency-dependent depolarization ratio $D^{2\nu_L(\nu)}$ of the He-Ne CIHR scattered light is also computed. The main results of the computations performed are presented and discussed in Sec. IV.

II. THEORY

A. Quantum spectra

Let us consider a system on which an intensive laser light wave of a frequency ω_L is incident. Then the HR scattering arises from the electric dipole moment proportional to the square of the electric field \mathbf{E} applied,

$$\mu_i^{2\omega_L} = \frac{1}{2} b_{ijk} E_i E_k, \quad (1)$$

where b_{ijk} is the hyperpolarizability tensor of the microsystem. Since the He and Ne atoms of the pair are spherical, no monomer double frequency induced dipole moment of the form as in Eq. (1) is expected. Conversely, however, the He-Ne pair has no center of symmetry. Therefore in a short time ($\approx 10^{-13}$ s) of a fly-by encounter of the colliding atoms forming the supermolecule, the collision-induced interatomic distance dependent hyperpolarizability $\mathbf{b}(R)$ emerges. As a result, according to Eq. (1) CI double frequency dipole moment $\mu_i^{2\omega_L}(R)$ is induced in the supermolecule being the origin of the CIHR scattering.

In our previous works of the series [32,34] on the hyper-Rayleigh scattering we defined the double differential intensity per supermolecule (diatom) scattered into a frequency $d\omega$ within a solid angle $d\Omega$ and normalized to the square of the intensity of the incident radiation I_0 (which will be from here on denoted as NDDI, i.e., normalized double differential intensity). The NDDI is a suitable quantity permitting a prediction and/or interpretation of the experimental CIHR spectra of mixtures of the noble gas atoms.

In this paper we compute and discuss the NDDI of CIHR spectra for the lightest pair of unlike noble gas atoms, namely for He and Ne. We consider a system of laboratory coordinates XYZ rigidly attached to the scattering medium. The incident light propagates in the direction of the Y axis and is polarized along the Z axis. Observation is assumed to be performed perpendicularly, along the X axis. As a consequence, the total scattered intensity can be divided into two components: a vertical (polarized) component $I_{ZZ}^{2\omega_L}$ and a horizontal one (depolarized) $I_{YZ}^{2\omega_L}$, defined in relation to the plane of observation. The corresponding components of NDDI are of the following form [34,37]:

$$\left(\frac{\partial^2 I_{AZ}^{2\omega_L}}{\partial \Omega \partial \omega} \right)_{HR} / I_0^2 = \frac{\pi}{2c} k_s^4 \sum_{i,i'} \rho_i | \langle i' | b_{AZZ} | i \rangle |^2 \delta(\omega - \omega_{i'i}), \quad (2)$$

where $\hbar \omega_{i'i} = E_{i'} - E_i$, ρ_i is the density-matrix element of the initial state i , and k_s stands for the wave vector of the HR

scattered light, moreover, $A=Z$ for the polarized component and $A=Y$ for the depolarized component. The wave functions of the relative motion of the two atoms of the supermolecule separated by the distance R are given by [38,39]

$$|i\rangle = |nlm\rangle = Y_{lm}(\hat{\mathbf{R}}) \frac{\Psi_i(R)}{R}, \quad (3)$$

where the angular part of the product is given by the spherical harmonic $Y_{lm}(\hat{\mathbf{R}})$, whereas $\Psi_i(R)$ is the radial wave function for state i .

Using the spherical tensor algebra methods we deal with the angular part of Eq. (2). Consequently the appropriate expression for the NDDI of the hyper-Rayleigh spectra for the polarized component reads [34]

$$\begin{aligned} & \left(\frac{\partial^2 I_{ZZ}^{2\omega_L}}{\partial \Omega \partial \omega} \right) / I_0^2 \\ &= \frac{\pi}{2c} k_s^4 \sum_{i,i'} \rho_i \left\{ (2l+1) \left[\frac{1}{5} H(1)'_i |(b_{10})'_i(E, \omega)|^2 \right. \right. \\ & \quad \left. \left. + \frac{2}{35} H(3)'_i |(b_{30})'_i(E, \omega)|^2 \right] \right\} \delta(\omega - \omega_{i'i}), \quad (4) \end{aligned}$$

whereas for the depolarized component we obtain

$$\begin{aligned} & \left(\frac{\partial^2 I_{YZ}^{2\omega_L}}{\partial \Omega \partial \omega} \right) / I_0^2 \\ &= \frac{\pi}{2c} k_s^4 \sum_{i,i'} \rho_i \left\{ (2l+1) \left[\frac{1}{45} H(1)'_i |(b_{10})'_i(E, \omega)|^2 \right. \right. \\ & \quad \left. \left. + \frac{4}{105} H(3)'_i |(b_{30})'_i(E, \omega)|^2 \right] \right\} \delta(\omega - \omega_{i'i}), \quad (5) \end{aligned}$$

where

$$(b_{k0})'_i(E, \omega) = \int_0^\infty \Psi_{i'}^*(R) b_{k0}(R) \Psi_i(R) dR \quad (6)$$

are the radial matrix elements of the spherical irreducible components $b_{k0}(R)$ ($k=1$ or 3) of the collision-induced molecular frame hyperpolarizability tensor [34]; $\Psi_i(R)$ is the radial wave function with energy E and the angular momentum quantum number l , whereas the $\Psi_{i'}(R)$ wave function corresponds to E' and l' , respectively. The spherical irreducible hyperpolarizability tensor rotational invariants b_{10} and b_{30} of Eqs. (4) and (5) are related to their b_1 and b_3 Cartesian counterparts [Eqs. (21) and (22)] by the following relations [7,34]:

$$b_{10} = -\sqrt{\frac{5}{3}} b_1, \quad b_{30} = \sqrt{\frac{2}{5}} b_3. \quad (7)$$

Moreover, using the 3- j Wigner symbols we obtain the following HR intensity factors:

$$H(k)_i^{l'} = (2l' + 1) \binom{l' \quad k \quad l}{0 \quad 0 \quad 0}. \quad (8)$$

We note that the $H(k)_i^{l'}$ coefficients can be directly compared to the $b_i^{l'}$ ones introduced by Placzek and Teller [40] for the linear scattering ($k=2$). Thus, according to Eqs. (5) and (6), for the depolarized component of the hyper-Rayleigh scattering we obtain

$$\begin{aligned} \mathcal{J}_{YZ}^{2\nu L}(\nu) &= V \left(\frac{\partial^2 I_{YZ}^{2\nu L}}{\partial \Omega \partial \nu} \right) / I_0^2 \\ &= \frac{\pi}{2} k_s^4 h L_0^3 \sum_l (2l+1) \left\{ \frac{1}{45} [H(1)_l^{l+1}(\mathcal{B}_{10})_l^{l+1}(\nu) \right. \\ &\quad + H(1)_l^{l-1}(\mathcal{B}_{10})_l^{l-1}(\nu)] + \frac{4}{105} [H(3)_l^{l+1}(\mathcal{B}_{30})_l^{l+1}(\nu) \\ &\quad + H(3)_l^{l-1}(\mathcal{B}_{30})_l^{l-1}(\nu) + H(3)_l^{l+3}(\mathcal{B}_{30})_l^{l+3}(\nu) \\ &\quad \left. + H(3)_l^{l-3}(\mathcal{B}_{30})_l^{l-3}(\nu)] \right\}, \quad (9) \end{aligned}$$

where L_0 is the thermal de Broglie wavelength of the relative motion of two atoms and V is the active scattering volume, moreover,

$$(\mathcal{B}_{k0})_i^{l'}(\nu) = \int_0^\infty dE e^{-\beta E} |(b_{k0})_i^{l'}(E, \nu)|^2; \quad (10)$$

and the bandwidths are measured in units of reciprocal centimeters. An analogous formula can be given for the polarized component [34]. One should also note that the double differential intensity of HR scattering is of the dimension $[(\partial^2 I_{YZ}^{2\nu L} / \partial \Omega \partial \nu)] = \text{erg cm}^{-1}$ (power irradiated per unit solid angle and per cm^{-1}). We shall use the above relations in the numerical calculations presented in the following parts of our work.

B. Classical spectra

We apply the standard procedure [38,41] previously presented in Ref. [34] in order to compute the classical trajectories of He-Ne colliding atoms, characterized at a time t by the polar coordinates $(R(t), \theta(t))$, for chosen interatomic potential [42] and for every possible value of b , the impact parameter, and s , the relative velocity of the encounter. Taking into account the free dimer trajectories, the Fourier transforms of the hyperpolarizability tensor components $[B_{10}(\nu, b, s)$ for the vector $b_{10}(R)$ and $B_{30}(\nu, b, s)$ for the septor $b_{30}(R)$], can be computed according to the method of Posch [43]:

$$B_{10}(\nu, b, s) = 4C_{1,1}(\nu, b, s) + 4S_{1,1}(\nu, b, s), \quad (11)$$

$$\begin{aligned} B_{30}(\nu, b, s) &= \frac{5}{2} C_{3,3}(\nu, b, s) + \frac{3}{2} C_{3,1}(\nu, b, s) + \frac{5}{2} S_{3,3}(\nu, b, s) \\ &\quad + \frac{3}{2} S_{3,1}(\nu, b, s), \quad (12) \end{aligned}$$

where (for k and $j=1$ or 3)

$$C_{k,j} = \left(\int_0^\infty b_{k0} [R(t, b, s)] \cos(2\pi\nu t) \cos[j\theta(t, b, s)] dt \right)^2, \quad (13)$$

$$S_{k,j} = \left(\int_0^\infty b_{k0} [R(t, b, s)] \sin(2\pi\nu t) \sin[j\theta(t, b, s)] dt \right)^2. \quad (14)$$

From these Fourier transforms, analogously to the formulas used for linear scattering and taking into account $G(\nu) = \exp[h\nu/(2k_B T)]$, the detailed balance correction, we derive in absolute units ($\text{cm}^8 \text{s erg}^{-1}$) the polarized $\mathcal{J}_{ZZ}^{2\nu L}(\nu)$ and the depolarized $\mathcal{J}_{ZY}^{2\nu L}(\nu)$ hyper-Rayleigh spectra scattered by a scattering volume V :

$$\mathcal{J}_{ZZ}^{2\nu L}(\nu) = \frac{1}{5} \mathcal{J}_{10}^{2\nu L}(\nu) + \frac{2}{35} \mathcal{J}_{30}^{2\nu L}(\nu), \quad (15)$$

$$\mathcal{J}_{ZY}^{2\nu L}(\nu) = \frac{1}{45} \mathcal{J}_{10}^{2\nu L}(\nu) + \frac{4}{105} \mathcal{J}_{30}^{2\nu L}(\nu), \quad (16)$$

where for the vector $k=1$ and the septor $k=3$ parts we have

$$\begin{aligned} \mathcal{J}_{k0}^{2\nu L}(\nu) &= \frac{\pi}{2} k_s^4 G(\nu) \\ &\quad \times \int_0^\infty s f_{MB}(s, T) 4\pi s^2 ds \int_0^\infty B_{k0}(\nu, b, s) 2\pi b db. \quad (17) \end{aligned}$$

In the latter, $f_{MB}(s, T) 4\pi s^2 ds$ stands for the Maxwell-Boltzmann factor. The corrected classical spectra defined by Eqs. (15)–(17) are numerically investigated for $T=295$ K and $T=95$ K in the next section.

III. NUMERICAL CONSIDERATIONS

In order to obtain the CI hyper-Rayleigh spectral profiles, the theoretical formulas from the previous sections should be supplemented with appropriate numerical procedures, either quantum mechanical or classical. In addition, at least two more necessary datasets are needed: first, the values of the hyperpolarizability tensors and their functional dependence on the intermolecular distance, and second, the potential curves characterizing the interactions of the atomic pairs considered. More complete information on the latter issues is given in the previous papers of the series (Refs. [32,34]) as well as in some earlier works (Refs. [44,45]), to which, and to the references thereof, the reader should refer for a more detailed description. In what follows we shall give mainly a brief outline of the chief facts and principles concerning the methods and the quantities of interest here.

A. Collisional hyperpolarizabilities

An extensive presentation of our computational methodology for interaction properties may be found in previous

TABLE I. Interaction anisotropy ($\Delta a/e^2 a_0^2 E_h^{-1}$) of the dipole polarizability and the vector ($b_1/e^3 a_0^3 E_h^{-2}$) and the septor ($b_3/e^3 a_0^3 E_h^{-2}$) part of the first dipole hyperpolarizability of He-Ne at the second-order Møller-Plesset level of theory. The He nucleus is on the negative z axis.

R/a_0	Δa	b_1	b_3	R/a_0	Δa	b_1	b_3
2.00	1.5690	9.07	-2.95	6.00	0.0974	-0.07	0.01
2.25	0.8096	3.90	0.69	6.50	0.0793	-0.03	0.02
2.50	0.4686	1.64	1.14	7.00	0.0646	-0.02	0.03
2.75	0.3071	0.54	0.98	7.50	0.0529	-0.01	0.03
3.00	0.2310	-0.02	0.71	8.00	0.0437	0.00	0.02
3.25	0.1970	-0.30	0.46	8.50	0.0365	0.00	0.02
3.50	0.1828	-0.42	0.27	9.00	0.0307	0.00	0.02
3.75	0.1766	-0.45	0.13	9.50	0.0261	0.00	0.01
4.00	0.1723	-0.43	0.04	10.00	0.0224	0.00	0.01
4.25	0.1670	-0.39	-0.01	11.00	0.0168	0.00	0.01
4.50	0.1598	-0.33	-0.04	12.00	0.0129	0.00	0.00
4.75	0.1508	-0.27	-0.04	13.00	0.0102	0.00	0.00
5.00	0.1405	-0.22	-0.03	14.00	0.0081	0.00	0.00
5.50	0.1184	-0.13	-0.01	15.00	0.0066	0.00	0.00

works (see Refs. [33,35,36]). A few essential details will be given here. We follow Buckingham's conventions and terminology throughout this section. In the finite-field method [46] the energy of an uncharged molecule in a weak and homogeneous static electric field can be written as

$$E^P = E^0 - \mu_\alpha F_\alpha - \frac{1}{2} a_{\alpha\beta} F_\alpha F_\beta - \frac{1}{6} b_{\alpha\beta\gamma} F_\alpha F_\beta F_\gamma - \frac{1}{24} c_{\alpha\beta\gamma\delta} F_\alpha F_\beta F_\gamma F_\delta + \dots, \quad (18)$$

where F_α, \dots is the field, E^0 is the energy of the free molecule, μ_α is the dipole moment, $a_{\alpha\beta}$ is the dipole polarizability, $b_{\alpha\beta\gamma}$ is the first dipole hyperpolarizability, and $c_{\alpha\beta\gamma\delta}$ is the second dipole hyperpolarizability. The subscripts denote Cartesian components and a repeated subscript implies summation over $x, y,$ and z . The number of independent components needed to specify the above tensors is regulated by symmetry. The mean and anisotropy of the polarizability and first hyperpolarizability are defined as

$$\bar{a} = \frac{1}{3}(a_{zz} + 2a_{xx}), \quad (19)$$

$$\Delta a = a_{zz} - a_{xx}, \quad (20)$$

$$b_1 = \frac{3}{5}(b_{zzz} + 2b_{zxx}), \quad (21)$$

$$b_3 = b_{zzz} - 3b_{zxx}. \quad (22)$$

The b_1 and b_3 rotational invariants of the first hyperpolarizability tensor are also considered as its vector and septor part, respectively.

The interaction electric properties of the heterodiatom are obtained via the well-tested Boys-Bernardi counterpoise-

correction (CP) method [47]. The interaction quantity $P_{\text{int}}(\text{He}\cdots\text{Ne})$ at a given internuclear separation R is computed as

$$P_{\text{int}}(\text{He}\cdots\text{Ne})(R) = P(\text{He}\cdots\text{Ne})(R) - P(\text{He}\cdots X)(R) - P(X\cdots\text{Ne}) \times (R). \quad (23)$$

The symbol $P(\text{He}\cdots\text{Ne})$ denotes the property P for He-Ne. $P(\text{He}\cdots X)$ is the value of P for the subsystem He in the presence of the ghost orbitals of subsystem Ne.

All properties were calculated at the self-consistent field (SCF) and second-order Møller-Plesset perturbation (MP2) level of theory [48]. We paid special attention to the choice of Gaussian-type basis functions (GTFs). We used large, flexible basis sets for our calculations: a $[6s4p3d1f]$ basis set for He and $[9s6p5d1f]$ for Ne, or 40 and 59 contracted GTFs. Details of their construction have been given in a previous paper [36]. Their quality is evidenced by the dipole polarizabilities calculated at the SCF level for the two atoms: $\alpha_{\text{He}} = 1.322$ and $\alpha_{\text{Ne}} = 2.368 e^2 a_0^2 E_h^{-1}$, to be compared with the numerical Hartree-Fock [49] values of 1.322 23 and 2.376 74, respectively. All electrons were correlated at the MP2 level. All calculations were performed with GAUSSIAN98 [50].

In Table I we show MP2 (full) values of the interaction polarizability and first hyperpolarizability of He-Ne for a large range of internuclear separations. In Figs. 1 and 2 we have plotted the R dependence of the mean and the anisotropy of the interaction hyperpolarizability at the MP2 levels of theory. Our results show that, from a computational point of view, the interest is mainly located in the relatively short internuclear separations. The change is rapid for all interaction properties. This is clearly the range where electron correlation and basis set effects are expected to be more important. Figure 3 shows the anisotropy of the computed interaction linear dipole polarizability of the He-Ne diatom.

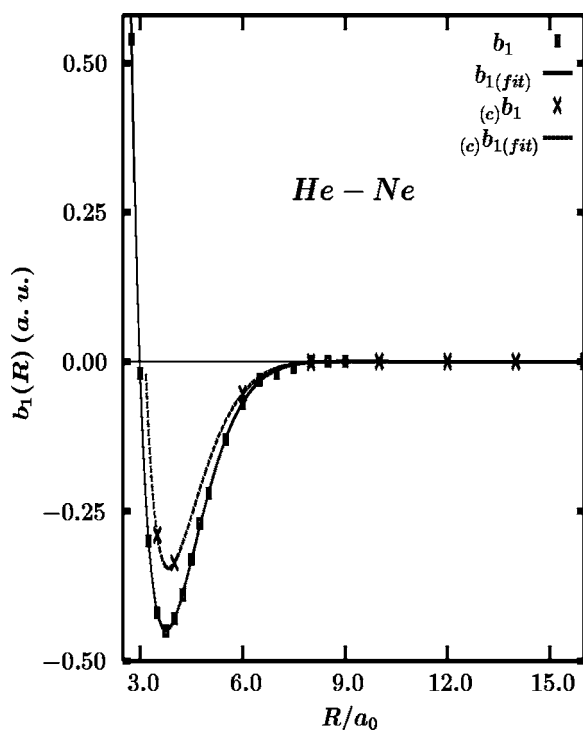


FIG. 1. The dipolar $b_1(R)$ hyperpolarizability component (in atomic units a.u.) vs the interatomic distance in units of Bohr (solid rectangles). The plot shows our results and the data of López Cacheiro *et al.* [42] (crosses; denoted by $(c)b_1$). The fitted functions are also shown ($b_{1(fit)}$). The lines are marked by the patterns indicated in the key section of the figure body.

We will not present extensively or discuss previous results in this paper, as it is clearly outside the scope of the present work. A detailed analysis of basis set and electron correlation effects will be reported elsewhere [51]. We mention a previous careful study by López Cacheiro *et al.* [42] who reported interaction dipole moment and (hyper)polarizabilities of He-Ne calculated at the CCSD level of theory. A more recent paper by Karamanis and Maroulis [52] reported CCSD(T) values of the interaction dipole moment and polarizability. They showed that high level electron correlation effects, as the addition of the triples to the CCSD treatment, are only important for very short internuclear separations.

The hyperpolarizability data are discrete sets of values and should be fitted to a functional analytical dependence, so that they could be used in our computing methods. It can be easily done by means of fitting functions of a relatively simple form of a sum of some exponential terms and inverse powers of the interatomic distance. The fitting procedure used is the well-known nonlinear least-squares Marquardt-Levenberg method [53].

B. Potential

The potential functions $\mathcal{V}(R)$ for the He-Ne systems were reported by several authors. Among them, those obtained by Cybulski and Toczyloski [54] (subsequently extended by Giese [55]) and by López Cacheiro *et al.* [42] are claimed to be the most accurate. In the present work we decide to imple-

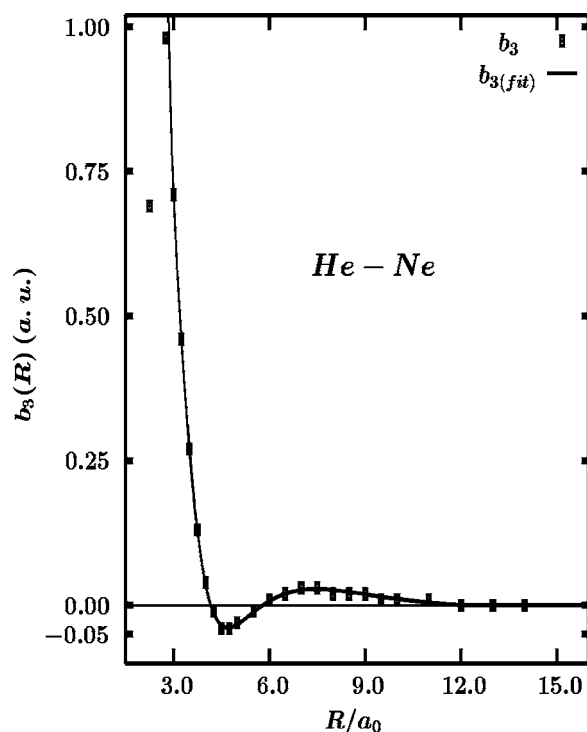


FIG. 2. The octopolar $b_3(R)$ hyperpolarizability component vs the interatomic distance (our results). The *ab initio* dataset points are denoted by the solid rectangles and the fitted function with the solid line.

ment the results of López Cacheiro's group, though the model given by Toczyloski and Cybulski has been also tested so that the two approaches could be compared. As a result we have found that the spectra computed by means of these methods do not differ substantially from those based on the model presented in Ref. [42], which therefore we have decided to be the only one considered in our calculations.

In the work by López Cacheiro *et al.* the original dataset is given in a tabular form, yet a functional expression fitting the *ab initio* numerical set is also provided. For obvious reasons—considering the nature of our calculations—the analytical formulas are the proper “input” here. In this approach the ten-parameter adjustable function introduced by Korona *et al.* [56] is applied so as to evaluate the potential

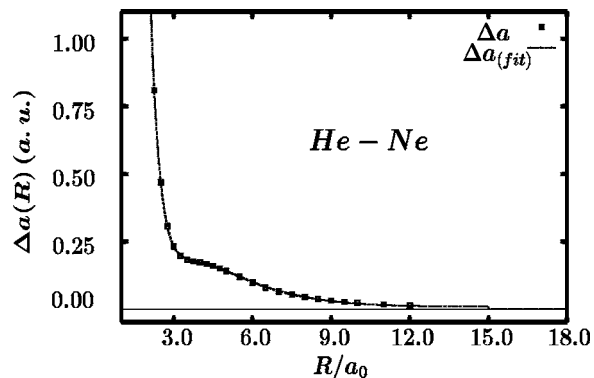


FIG. 3. The anisotropy of the linear dipole polarizability of He-Ne diatom vs the interatomic distance (our *ab initio* results).

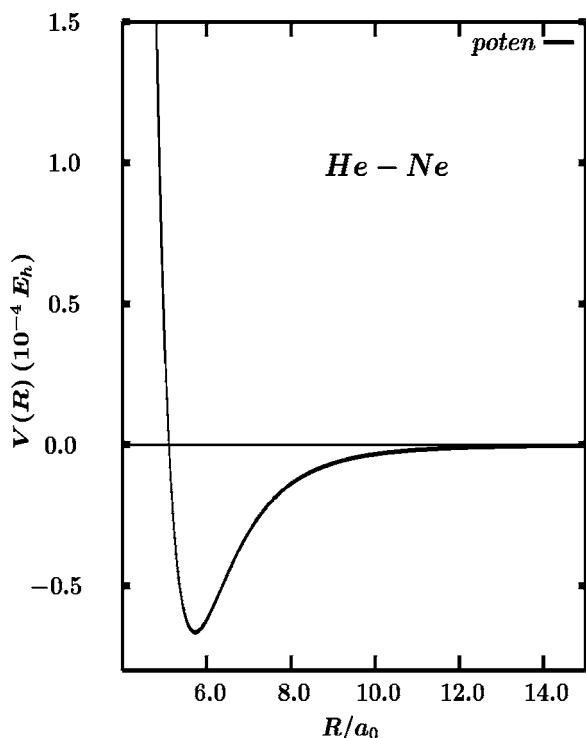


FIG. 4. The interaction potential for He-Ne diatom after Ref. [42].

dependence on R , the fitting parameters being given in Ref. [42]. As a result a potential curve is found with the minimum value within the attractive well: $\varepsilon = -6.654 \times 10^{-5} E_h$ at $r_m = 5.435 a_0$ and with $\mathcal{V}(R) = 0$ at $\sigma = 5.101 a_0$. The shape of the potential is visualized in Fig. 4.

C. Calculations

1. Quantum approach

In the quantum-mechanical formulas for the collisional spectrum in Eqs. (4) and (5) all the matrix elements there may be evaluated on the condition that the radial wave functions of a system of colliding atoms are at hand. Consequently, as these functions are a solution of the radial Schrödinger equation, we inevitably have to apply an appropriate numerical procedure of solving it. The method to achieve this goal, implemented in the preceding papers of the series, can be well adopted to the present work tasks. Admittedly though, the computing workload for relatively less massive pairs of atoms, such as He and Ne, is far less a burden than that for the previously analyzed Kr-Xe case. Thus the advantages of the code applied in earlier works might not be so crucial for the present jobs. Yet, we have decided to introduce it in this work as it is a procedure that has been checked and proven reliable in many computations before.

The algorithm of the method is based on integrating a differential equation, and then evaluating the integrals in the matrix elements in Eqs. (4) and (5) along a contour defined in the complex plane. In the case of the heavier atoms it allows bypassing the cancellation-oscillation errors appear-

ing when matrix elements are to be calculated without excessive extension of the number of the integration points. In the procedure applied, the Numerov method [57] is used in order to find the desired solutions of the Schrödinger equations, with the WKB functions [58] used to estimate the initial points of the integration and to provide normalizing factors. The more thorough description of the particular steps of the calculations is presented in several earlier works and the references there; see, e.g., Refs. [44,45,59].

The scope of the parameters of integration that are to be used so that convergent and precise final results should be received is for the He-Ne pairs less restrictive than for Kr-Xe: the sufficient value of the maximum l quantum number is about 60 in the case of the b_1 component of the spectrum and about 150 for the b_3 contribution (for Kr-Xe the numbers are about 200 and 400, respectively). As for the initial energies needed to evaluate convergent integrals, their values vary from 0.002ε to 230ε , and the lower limit of intermolecular distances should start from $R = 2.8 a_0$ for the vector, and from $R = 3.2 a_0$ for the septor profiles. The upper limit of integration and the grid of R was set at $R = 55.0 a_0$ and 10 000 points, respectively. Though, it must be stressed here that, as a matter of fact, these estimations might have been excessively pushed to extreme levels, and according to our assessment they might well be reduced substantially with little or next to no loss of accuracy.

With so determined sets of the quantities and parameters involved in the computing process, the code used produces a spectral profile comprising 320 points within the CPU time of order of 1 h for b_1 and 5 h for b_3 on a two-processor (Pentium IV, 2.8 GHz) machine. However, these relatively large estimates are obtained for highly demanding accuracy requirements. Thus if a slightly lower regime of precision is accepted, the time of calculation may be reduced considerably, even at the rate of 5, which could be an important asset of the code, when a numerous series of experimental profiles has to be interpreted fast and efficiently *on line*.

In this work the resulting spectral profiles obtained by means of the above-mentioned procedure are presented in Figs. 5 and 6. They will be discussed in a more detailed manner in the last section of the study.

Continuing our considerations in the following sections, we shall also apply the zeroth spectral moments as a verification device used, first of all to check the validity of the computed profiles and, on the other hand, in order to compare the quantum and classical approach.

These moments of the scattered HR light spectra and the contributions to them associated with the particular components of the hyperpolarizability tensor can be obtained from the spectral profile, according to their definition [39]:

$$M_0^{b_{k0}} = \frac{2c}{\pi} \left(\frac{4\pi}{\lambda_L} \right)^4 \int_{-\infty}^{+\infty} \mathcal{J}_{k0}^{2\nu_L} d\nu, \quad (24)$$

where λ_L denotes the wavelength of the laser light. In our computations we assumed $\lambda_L = 514.5$ nm.

Alternatively, these quantities may be calculated by means of the formulas applying the pair correlation function $g(R)$. According to Refs. [34,39], the appropriate expression

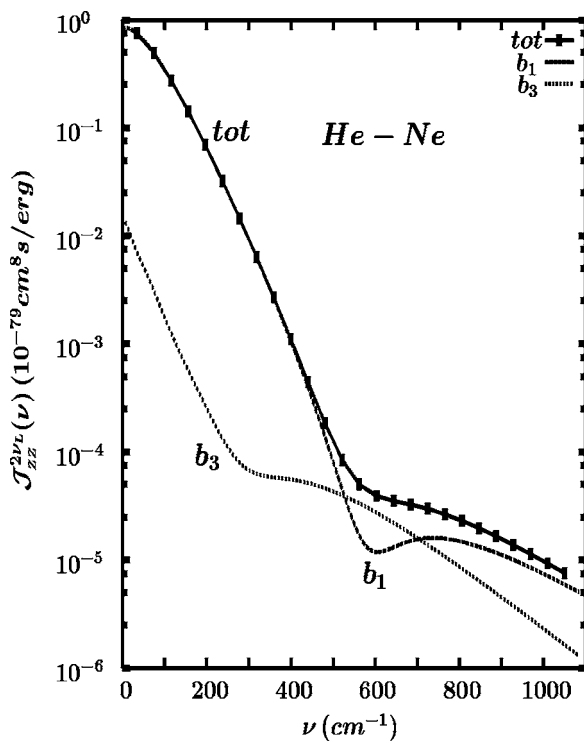


FIG. 5. The polarized CI hyper-Rayleigh $\mathcal{J}_{ZZ}^{2\nu}(\nu)$ light scattering spectrum for He-Ne pairs at $T=295$ K (quantum-mechanical results). The normalized double differential intensity (labeled by *tot*) is given in the absolute units (see the text). They are supplemented by the diagrams illustrating the contributions to the total spectra yielded by the hyperpolarizability vector (b_1) and septor (b_3) parts.

for the zeroth moment (sum rule) is of the shape

$$M_0^{b_{k0}} = 4\pi \int_0^\infty b_{k0}^2(R)g(R)R^2 dR. \quad (25)$$

The equilibrium pair-correlation function can be derived within the quantum approach by the following expression:

$$g(R) = \frac{V}{\mathcal{Z}} \langle \mathbf{R} | \exp(-\beta\mathcal{H}) | \mathbf{R} \rangle, \quad (26)$$

where \mathcal{Z} is the partition function for the relative motion of the atoms of the supermolecule in a box of volume V . The system dynamics is determined according to the Hamiltonian \mathcal{H} :

$$\mathcal{H} = \frac{p^2}{2\mu} + \mathcal{V}(R), \quad (27)$$

with μ denoting the reduced mass of two colliding particles. On applying appropriate procedures of the quantum mechanics we can derive from these equations an expression determining the pair-correlation function in a form suitable for numerical computations:

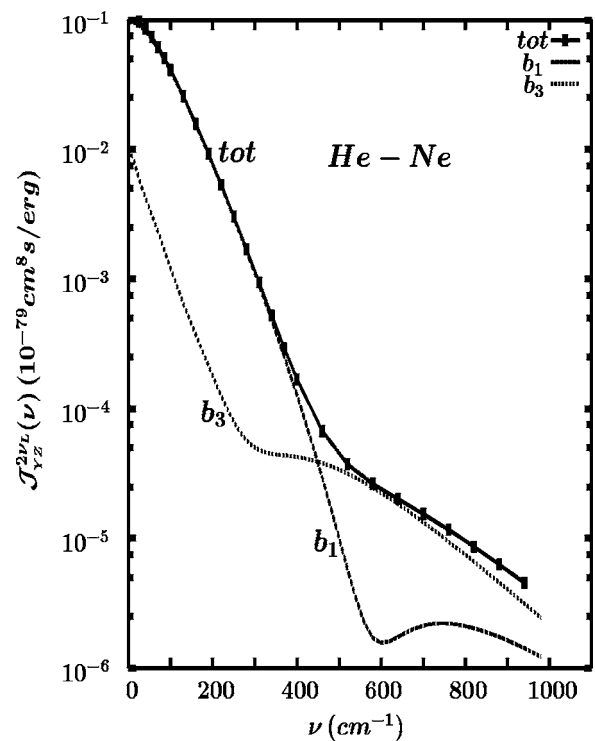


FIG. 6. The same as in Fig. 5 but for the depolarized component (classical results).

$$g(r) = \frac{L_0^3 \mu^{3/2}}{2^{1/2} \pi^2 \hbar^3} \sum_{l=0}^{\infty} \int_0^\infty dE E^{1/2} \exp[-\beta E] \mathcal{R}_{El}^*(R) \mathcal{R}_{El}(R), \quad (28)$$

where $\mathcal{R}_{El} = \Psi_{El}(R)/R$, and $\Psi_{El}(R)$ is a solution of the radial Schrödinger equation for the system considered. Fortunately, a precise code needed in order to obtain the wave functions \mathcal{R}_{El} can be derived with far less difficulty than the one which is used for calculating the spectral profiles [44]. Now, we deal with merely the \mathcal{R}_{El} squared and, as a result, the problem of the error due to the cancellation-oscillation effect becomes negligible. Therefore the Schrödinger equation for the systems considered may be solved without having recourse to the highly sophisticated algorithms like the one we use in the spectral considerations: integration simply along the real axis seems quite sufficient in this case yielding a very accurate outcome within relatively short CPU time used. The comparison between the integrated intensities resulting from the computed quantum HR profiles, Eq. (24), and from the sum rule formula, Eq. (25), together with the quantum pair-correlation function, Eq. (28), is given in Table II.

2. Classical approach

For heavy molecular systems and for relatively high temperatures, classical and quantum-mechanical calculations of CIHR spectra are expected to give similar results. It has been recently checked for the Kr-Xe HR spectra at $T=295$ K [34]. In such a case, classical and quantum-mechanical pair correlation functions are very close to each other for any value of R , the distance separating molecules or

TABLE II. The quantum-mechanical integrated intensities [according to Eq. (24)] calculated from the spectral profile contributions, related to the b_{k0} ($k=1,3$) tensorial components (M^{FS}), compared with their counterparts (M^F) obtained by means of the quantum sum-rule formula [Eq. (25)]; free dimer case. The quantities are expressed in $\text{cm}^{12} \text{erg}^{-1}$.

	$T(\text{K})$	M_0^F	M_0^{FS}	M_0^F/M_0^{FS}
b_{10}	95	2.609×10^{-88}	2.571×10^{-88}	1.0140
	295	3.909×10^{-88}	3.923×10^{-88}	0.9964
b_{30}	95	1.220×10^{-89}	1.209×10^{-89}	1.0091
	295	1.222×10^{-89}	1.230×10^{-89}	0.9983

atoms. However, for light systems such as He-Ne, much more attention must be paid to purely quantal contributions, as they possibly can have a substantial influence on the absolute intensities as well as on the spectral profiles of the corresponding HR spectra. At the first approximation, Wigner has shown that the pair-correlation function may be expanded at intermediate temperatures in even powers of the Planck constant [60]. If \mathcal{V} , the intermolecular potential, depends only on R , the expansion up to \hbar^2 of the pair-correlation function is defined by [61]

$$g_2(R) = g_0(R) \left\{ 1 + \frac{\hbar^2}{12\mu(k_B T)^2} \left(\frac{\mathcal{V}'^2}{2k_B T} - \frac{2\mathcal{V}'}{R} - \mathcal{V}'' \right) \right\}, \quad (29)$$

where $g_0(R) = \exp[-\mathcal{V}/(k_B T)]$ is the classical pair-correlation function, whereas the symbols ' and '' stand for the first and the second R derivatives, respectively. The reliability of the classical pair-correlation function may be easily checked from its comparison with the values of $g_2(R)$. Let us consider, for example, the value of the difference $|g_2(R) - g_0(R)|$ at its maximum, found for the interatomic distance R_M . The ratio $\rho = |g_2(R_M) - g_0(R_M)| / g_0(R_M)$ provides an order of magnitude of the quantum-mechanical corrections introduced by Eq. (29) relative to the classical pair-correlation function. Moreover, in contrast to the often applied mean square root, ρ does not depend on any range of R considered. For the potential of the pair Kr-Xe given in Ref. [62], $\rho \leq 0.3\%$ at room temperature and $\rho \leq 1\%$ beyond 95 K; below 75 K, $\rho \geq 10\%$. Note that, for significantly low temperatures, neither $g_0(R)$ nor $g_2(R)$ are accurate anymore

because the Wigner expansion up to \hbar^2 remains valid for corrections of a few percent only. In the case of the He-Ne pair, and for the potential proposed recently in Ref. [42], $\rho = 3\%$ at 295 K and $\rho > 10\%$ below 120 K. This is ten times the corresponding values of ρ found for the Kr-Xe pair. However, at $T = 295$ K, the quantum-mechanical corrections remain relatively low. In conclusion, a classical approach may still be used to calculate CIHR spectra of the pair He-Ne at room temperature, as long as the acceptable error should not fall below the aforementioned percentage estimations.

The classical spectral profiles are computed by means of a numerical evaluation of Eqs. (15)–(17). In order to perform a verification of their reliability, the classical spectral zeroth moment (integrated intensities) has been calculated according to

$$M_0^{b_{k0}} = \frac{2c}{\pi} \left(\frac{4\pi}{\lambda_L} \right)^4 \int_{-\infty}^{\infty} \mathcal{J}_{k0}^{\nu_L}(\nu) G(\nu)^{-1} d\nu. \quad (30)$$

On the other hand, the classical zeroth moment corresponding to the vector ($k=1$) and the septor ($k=3$) components of the hyperpolarizability tensor must be equal to the classical canonical average:

$$M_0^{b_{k0}} = V \langle b_{k0}^2(R) \rangle, \quad (31)$$

where $\langle \dots \rangle$ denotes the low-density mean value:

$$\langle f(R) \rangle = \frac{1}{V} \int_0^\infty f(R) g_0(R) 4\pi R^2 dR. \quad (32)$$

We should be aware, however, that in our classical intensities $\mathcal{J}_{k0}(\nu)G(\nu)^{-1}$ we take into account the free dimer contribution only and not the contribution of the bound and metastable pairs. Therefore prior to any numerical comparison between results of Eq. (30) and those of Eqs. (31) and (32), every moment involved given by the above-mentioned canonical averages must be multiplied by x_0^k , a part of the moment due to the free dimers. The dimensionless factors x_0^k can be calculated by using the classical method of Levine [63]. In the case of He-Ne at $T = 295$ K, they are roughly equal to 1, because the potential well depth is 15 times lower than $k_B T$ and the intensity contribution due to bound and metastable dimers is negligible. Conversely, at very low temperatures, x_0^k can be significantly lower than 1. Taking into account these correction factors, it can be checked in Table III that the results of Eq. (30) are fully compatible with those

TABLE III. Comparison between the integrated intensities $M_0^{b_{k0}}$ of the HR spectra due to free dimers He-Ne and related to components b_{k0} ($k=1,3$) of the hyperpolarizability tensor and the corresponding sum-rule result $x_0^k V \langle b_{k0}^2 \rangle$. The integrals $M_0^{b_{k0}}$ and $V \langle b_{k0}^2 \rangle$ are expressed in $\text{cm}^{12} \text{erg}^{-1}$. The ratios x_0^k giving intensity portions due to the free dimers are dimensionless.

	$T(\text{K})$	M_0	x_0^k	M_0^F	M_0^{FS}	M_0^F/M_0^{FS}
b_{10}	95	2.734×10^{-88}	0.968	2.645×10^{-88}	2.634×10^{-88}	1.004
	295	4.002×10^{-88}	0.996	3.987×10^{-88}	3.960×10^{-88}	1.007
b_{30}	95	1.243×10^{-89}	0.985	1.225×10^{-89}	1.222×10^{-89}	1.002
	295	1.247×10^{-89}	0.997	1.244×10^{-89}	1.236×10^{-89}	1.006

of Eqs. (31) and (32) for $T=95$ K and $T=295$ K. This confirms the internal coherence of our classical calculations, at least for the region of the frequencies for which the intensities give the most decisive contribution to the zeroth moment (up to ≈ 250 cm^{-1}).

Moreover, it might be noticeable that the computation of the zeroth moments can be useful so as to evaluate the feasibility of the CIHR experiment for given experimental con-

ditions. To this end it is possible to compare the integrated intensity of the He-Ne CIHR spectrum and the integrated intensity of allowed HR radiation scattered by a simple system composed of heterogeneous diatomic molecules. The spectral distribution of the polarized component of the He-Ne HR scattered light, *per unit volume irradiated* (p.u.v.), is given by

$$\frac{1}{I_0^2} \left(\frac{\partial^2 I_{ZZ}^{2\nu_L}(\mathbf{p} \cdot \mathbf{u} \cdot \mathbf{v} \cdot)}{\partial \Omega \partial \nu} \right)_{\text{He-Ne}} = \underbrace{\frac{N_{\text{He}} N_{\text{Ne}}}{V}}_{\text{density of diatoms}} \left(\frac{\partial^2 I_{ZZ}^{2\nu_L}}{\partial \Omega \partial \nu} \right)_{\text{He-Ne}} \Big/ I_0^2 = n_{\text{He}} n_{\text{Ne}} V \left(\frac{\partial^2 I_{ZZ}^{2\nu_L}}{\partial \Omega \partial \nu} \right)_{\text{He-Ne}} \Big/ I_0^2, \quad (33)$$

where n_i denotes the partial number density of an atomic mixture component i . For He-Ne mixture we compute the unit volume integrated CIHR intensity using the zeroth spectral moments, M_0^{FS} given in Table II. As a result we have

$$\frac{1}{I_0^2} \left(\frac{\partial I_{ZZ}^{2\nu_L}(\mathbf{p} \cdot \mathbf{u} \cdot \mathbf{v} \cdot)}{\partial \Omega} \right)_{\text{He-Ne}} = n_{\text{He}} n_{\text{Ne}} \frac{\pi}{2c} k_s^4 \left\{ \frac{1}{5} M_0^{FS}(b_{10}^{\text{He-Ne}}) + \frac{2}{35} M_0^{FS}(b_{30}^{\text{He-Ne}}) \right\}. \quad (34)$$

On the other hand, as far as we consider the polarized allowed HR integrated intensity scattered per unit volume of a gas X we have

$$\frac{1}{I_0^2} \left(\frac{\partial I_{ZZ}^{2\nu_L}}{\partial \Omega} \right)_X = n_X \frac{\pi}{2c} k_s^4 \left\{ \frac{1}{5} |b_{10}^X|^2 + \frac{2}{35} |b_{30}^X|^2 \right\}, \quad (35)$$

where b_{k0}^X stands for the molecule frame hyperpolarizability tensor of the molecules X and n_X is their number density. Considering for example the HF molecule, the relevant hyperpolarizability tensor components, in atomic units are [64] $b_{10} = 7.23$ a.u. and $b_{30} = -4.49$ a.u. Applying these values for the allowed spectra at $T=295$ K we calculate the ratio

$$\begin{aligned} & \frac{(\partial I_{ZZ}^{2\nu_L} / \partial \Omega)_{\text{He-Ne}}}{(\partial I_{ZZ}^{2\nu_L} / \partial \Omega)_{\text{HF}}} \\ &= \frac{n_{\text{He}} n_{\text{Ne}} \left((1/5) M_0^{FS}(b_{10}^{\text{He-Ne}}) + (2/35) M_0^{FS}(b_{30}^{\text{He-Ne}}) \right)}{n_{\text{HF}} \left((1/5) |b_{10}^{\text{HF}}|^2 + (2/35) |b_{30}^{\text{HF}}|^2 \right)} \\ &= 2.46 \times 10^{-6} \frac{\rho_{\text{He}} \rho_{\text{Ne}}}{\rho_{\text{HF}}}, \end{aligned} \quad (36)$$

where ρ_i denotes the density of the species i in amagats.

IV. RESULTS, DISCUSSION, AND CONCLUSION

In this work we have investigated the CI hyper-Rayleigh type of light scattering in the media consisting of the diatomic He-Ne supermolecules. Both quantum and classical calculations have been performed based on the theoretical

background previously developed in Refs. [32,34], and applying the datasets obtained for the collisional hyperpolarizabilities by means of the *ab initio* methods elaborated by the group of Maroulis and referred in Sec. III. Two temperature conditions have been taken into account in order to compare the quantum and classical profiles as, unlike in the case of the more massive supermolecules Kr-Xe studied before [34], it is usually expected that for lighter systems (such as He-Ne) the quantum nature of the processes in which they are involved may turn out to be more significant. In addition, the zeroth spectral moments (the integrated intensities) of the spectra have been evaluated and used as a criterion of the reliability of the profiles computed.

The resulting profiles are presented in Fig. 5, where the intensities of the polarized ZZ component of the scattered light are shown, and in Fig. 6 with the depolarized YZ spectral line visualized in it. They are supplemented by diagrams illustrating the contributions to the total spectra yielding by the hyperpolarizability vector (b_1) and septor (b_3) parts.

In these pictures there are some noticeable features of the spectra worth mentioning. First, it should be noted that the absolute intensities in the system considered are by far smaller than those obtained for the Kr-Xe pairs, with their maximum values of five orders of magnitude lower. The peak-to-wing ratio, within the frequency range assumed, on the other hand, is quite similar for the two systems, reaching in the He-Ne case the value of approximately 10^5 for the ZZ profile and a little less than this for the YZ one. One must be aware, however, that the frequency range is now much larger: 1000 cm^{-1} compared with 350 cm^{-1} for Kr-Xe.

Second, the difference between the Kr-Xe and He-Ne spectra is also clearly visible when comparing their initial (beyond the most low-frequency limit) slopes, Δ : for He-Ne we obtain $\Delta=48$ cm^{-1} vs $\Delta=16$ cm^{-1} for Kr-Xe. Considering the shape of the profiles, it could be also useful to point out that for He-Ne in a very rough description a single relatively sharp exponential function with a gradually curving slope of approximately ($\Delta=48$ cm^{-1}) represents the He-Ne spectrum up to 600 cm^{-1} and at the very far wings

($\nu > 600 \text{ cm}^{-1}$) the line falls off much more slowly with $\Delta = 200 \text{ cm}^{-1}$. This description holds in particular for the depolarized intensities.

Eventually, we should pay attention to some characteristic features that the two molecular spectra (Kr-Xe and He-Ne) have in common. As one studies the influence on the resulting profiles which are brought about by the two tensorial mechanisms related to the b_1 and b_3 components, they can easily arrive at a conclusion that also for the He-Ne systems the vector part share prevails within a relatively large range of frequencies. It should be remarked however, that—contrary to the Kr-Xe pairs—the contribution introduced by b_3 is slightly more spectacular within certain sectors of the He-Ne spectra. From Fig. 5, showing the polarized $\mathcal{J}_{ZZ}^{\nu}(\nu)$ hyper-Rayleigh spectrum, it is evident that up to about 420 cm^{-1} the entire spectrum originates from the $b_1(R)$ contribution. Then, in the region between 500 and 700 cm^{-1} , the $b_3(R)$ component becomes increasingly important reaching its maximum value at about 600 cm^{-1} , and again for the frequencies larger than 700 cm^{-1} the $b_1(r)$ hyperpolarizability influence predominates. That prevalence of the septor collisional effect at the high frequencies (above $\approx 400 \text{ cm}^{-1}$) is even more profound in the total depolarized $\mathcal{J}_{YZ}^{\nu}(\nu)$ spectrum, where it almost exclusively shapes the far wings. This situation partially stems from the values of the geometrical weight coefficients [Eqs. (4) and (5)], which for the depolarized component are equal $1/45$ vs $4/105$, while for the polarized light their counterparts are $1/5$ and $2/35$ (for the b_1 and b_3 contributions, respectively).

In Fig. 7 (mind the linear scale) the He-Ne CI depolarized Rayleigh spectrum and the b_1 and b_3 contributions to the HR scattering are compared, all being normalized to the same value at zero frequency. We note that the vector part of the HR spectrum decreases most slowly with frequency, its half width at half maximum (HWHM) being equal to approximately 90 cm^{-1} , whereas the Rayleigh spectrum is the narrowest one with HWHM of about 20 cm^{-1} . The septor part of the HR spectrum locates in between reaching the HWHM of about 30 cm^{-1} . It is worth noticing that there is no evident correlation between the rank k of the tensors involved: b_1 , Δa_2 , and b_3 and the HWHM corresponding to their appropriate spectral contributions, which is contrary to the one-molecule scattering, in which—according to the rotational molecular diffusion model, $\text{HWHM} \approx k(k+1)$ Ref. [7]. This is because in the CI case, the width of the spectral lines should be rather compared to the inverse of the maximum range of the respective CI light scattering mechanism (meaning the distances at which the values of the appropriate tensor components considerably differ from zero). In other words, we should take into account the reciprocal of the time of the effective collisions in order to assess the value of HWHM. When examining Fig. 3, we observe that the R dependence of the CI linear polarizability anisotropy, Δa_2 , is of the longest range, whereas the range of b_1 is the shortest, and what is more—this component of \mathbf{b} decays with R most rapidly of all the studied tensors. In conclusion we may therefore notice that, as far as the HWHM is concerned, the spectra studied here follow the regularity previously observed in the case of the collision-induced: absorption and linear light scattering [38,39].

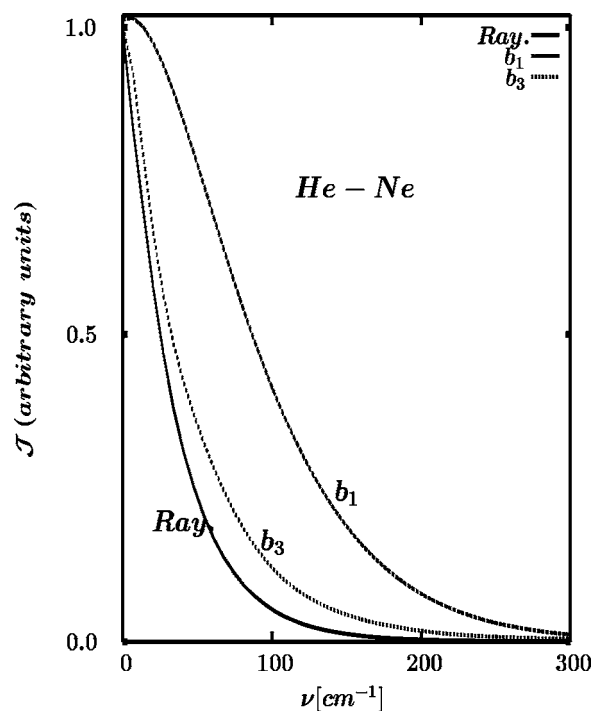


FIG. 7. The purely collision-induced depolarized Rayleigh (*Ray*) light scattering spectrum of the He-Ne pair computed with the linear polarizability anisotropy presented in Fig. 3 vs the hyper-Rayleigh spectrum components (b_1 and b_3) computed for the same temperature and for the same *ab initio* calculation model. The spectral lines have been adjusted in order to match the same value at $\nu=0$.

The other feature typical of both the Kr-Xe and He-Ne profiles is the presence of characteristic bents “spoiling” the monotonic decay of the b_1 and b_3 origin profiles and consequently finding their reflection in the similar features observed in the total spectra. This kind of behavior was reported by several authors in their works on the collisional Rayleigh scattering [65–67], where it was attributed to the pattern which the dependence of the polarizability on the intermolecular separation follows. When interpreting our results, we feel inclined to such a thesis as, according to our analysis, the bents do originate from the short and midrange properties of $b_k(R)$, mainly from the minima and maxima which are there within the small distances available for the colliding atoms to penetrate. In this context it is worth pointing out that this functional behavior of $b_k(R)$ in our case results not from any artifact of a numerical tool applied, but from the *ab initio* calculations based on solid and physically justifiable models from which the collisional hyperpolarizabilities are evaluated [33,42]. An additional consequence of the above notion might be that, once the experimental results for the effects discussed in this work are available, our profiles might serve as a benchmarking device to assess the validity of the physical assumptions applied in the *ab initio* computations.

Furthermore, in this work, we have also analyzed the frequency-dependent depolarization ratio of the studied spectra, as it is one more quantity that plays an important role in description and discussion spectral properties, obtained both

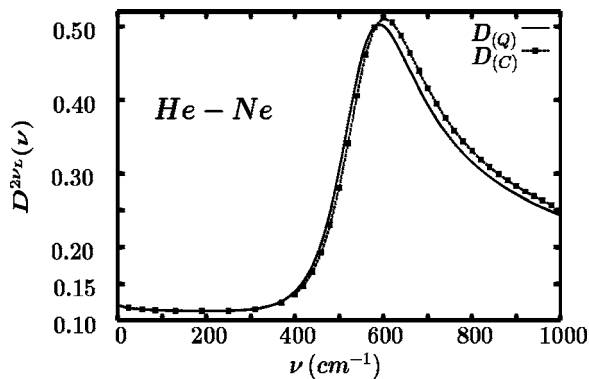


FIG. 8. The frequency-dependent depolarization ratio $D^{2\nu_L}(\Delta\nu)$ computed for the linearly polarized incident light and for the collection light scattered optics applying analyzer. The results of quantum (Q) and classical (C) computations are shown as indicated by the key symbols in the right top corner of the figure.

experimentally as well as theoretically. In this study it offers an additional possibility of assessing the relative participation of the b_1 and b_3 contributions in forming the resulting HR spectra.

In Fig. 8 we show the frequency-dependent depolarization ratio $D^{2\nu_L}(\nu)$ calculated for the linearly polarized incident light and for collecting light scattered optics applying analyzer defined as

$$D^{2\omega_L}(\Delta\nu) = \frac{I_{YZ}^{2\omega_L}(\Delta\nu)}{I_{ZZ}^{2\omega_L}(\Delta\nu)} = \frac{(1/45)|b_{10}(\Delta\nu)|^2 + (4/105)|b_{30}(\Delta\nu)|^2}{(1/5)|b_{10}(\Delta\nu)|^2 + (2/35)|b_{30}(\Delta\nu)|^2}. \quad (37)$$

We note that in the frequency range 0–400 cm^{-1} , where the vector component predominates, the depolarization ratio is close to the theoretical value of 1/9 typical of the pure-vector-type collisional mechanism [32]. Then, in the frequency range 400–800 cm^{-1} where the septor hyperpolarizability component contribution to the spectrum prevails, $D^{2\nu_L}(\nu)$ heads towards its theoretical “septor only” value of 2/3 reaching its maximum value equal ≈ 0.50 at $\nu \approx 600 \text{ cm}^{-1}$, where it starts to decrease in value again due to the diminishing importance of the septor part of the hyperpolarizability tensor. This rather dramatic increase in the theoretical value of $D^{2\nu_L}(\nu)$, if observed experimentally, might serve as an evidence of a possibly important septor share in the overall picture of the scattering process studied.

One of the aims of the reported project and a question that has been addressed is the problem of assessment to what extent and on what condition a supermolecule taking part in the HR scattering processes must be treated as a quantum system, and when it is allowed to be described classically. It seems that for the least massive noble gas atomic pairs at room and higher temperature the classical approach is supposed to be sufficient in many cases, which is usually claimed in literature [38,39]. Nevertheless, even in such circumstances one may expect a non-negligible influence of the quantum corrections, and even more so at significantly lower temperatures.

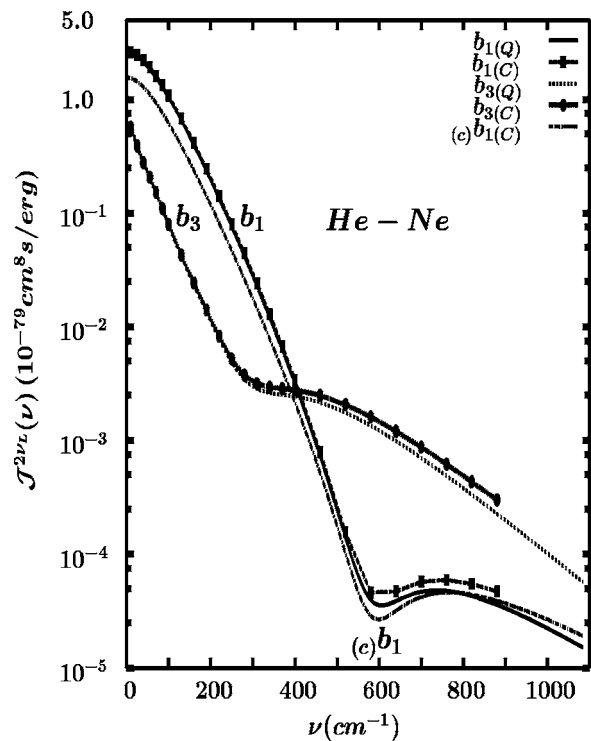


FIG. 9. The comparison between the quantum (Q) and the classical (C) profiles due to the b_1 and b_3 parts of the HR spectrum for 295 K. Additionally the b_1 component of the HR spectrum based on López Cacheiro *et al.*'s dataset is given here (labeled with $(c)b_1$ in the figure body). See the keys of the lines in the top-right corner of the figure.

The calculations reported in the above sections bring forth two sets of results: the one that stems from the quantal theory and the other obtained by means of the classical analytical and numerical tools. The profiles plotted in Fig. 9 illustrate the difference between the quantum and classical lines resulting from the two collisional mechanisms: b_1 and b_3 (at $T=295 \text{ K}$).

Additionally, in the same figure, for comparison, there is also a profile computed on the grounds of the data provided in Ref. [42] and labeled with $(c)b_1$ in the figure body. The shape of the graph resembles the line resulting from the $b_1(R)$ values reported in our work, while the intensities differ considerably. The latter comes as no surprise as the $b_1(R)$ functions for the two cases are not identical as well (see Fig. 1). Furthermore, the range of $b_1(R)$ obtained in Ref. [42] does not reach far enough towards the short R distances. In fact, both the qualitative agreement of the profile rendered from these data with the one obtained in within our study, as well as the convergence of the computed spectrum were only possible at the expense of an additional extrapolation applied (the left-most section of the dashed line of Fig. 1). Otherwise the two spectra would be dramatically apart from one another, especially at the wings. The above observation can be one more evidence of the importance of the short-range behavior of $b_1(R)$ for shaping the analyzed spectra.

Having compared the spectra in Figs. 9 and 10, we find that indeed, unlike in the case of more massive Kr-Xe pairs,

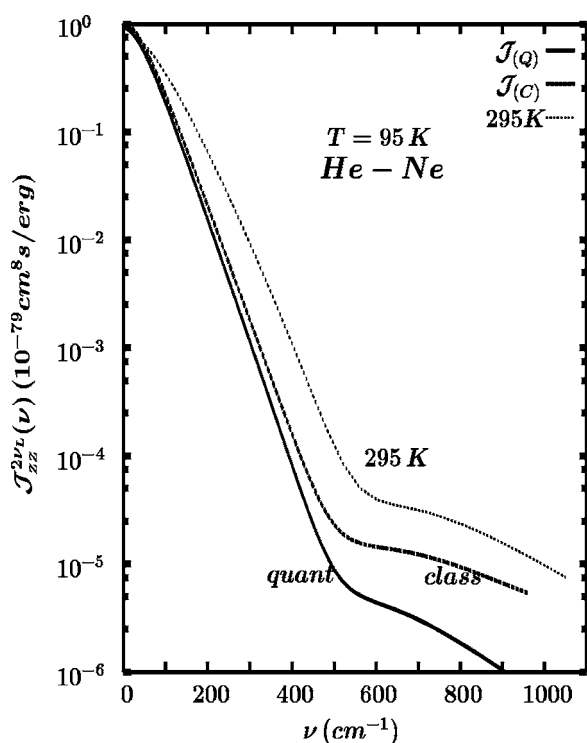


FIG. 10. The quantum-mechanical (quant) and classical (class) polarized hyper-Rayleigh $\hat{J}_{ZZ}^{2\nu}(\nu)$ light scattering spectra for He-Ne pairs at $T=95$ K. The quantum-mechanical results for 295 K are also plotted for comparison.

in the He-Ne systems the discrepancy between the spectral properties determined within the quantum and the classical approach cannot be treated as negligible. Although at the room temperature the spectral profiles of classical and quantum origin virtually seem almost the same—especially when plotted in the semilogarithmic scale—more thorough analyzes reveals that the difference between them is in fact systematic. In the region close to the very center of the profiles the deviation is of the order of approximately 2.5% (both for the b_1 and the b_3 components) and grows to 6.0% and 4.5%, for b_1 and b_3 , respectively, at $\nu \approx 250$ cm^{-1} ; this frequency marks the upper limit for the part of the spectrum that gives the preponderant contribution to the zeroth spectral moments. However, as we follow along the spectra towards the higher frequencies, the quantum-mechanical and the classical spectra start to diverge conspicuously to reach eventually $\approx 20\%$ of discrepancy for $\nu \approx 900$ cm^{-1} . In conclusion, the quantum nature of the processes considered, though not especially predominant at higher temperatures, even then should not be treated as negligent in systems such as He-Ne.

All the more so, this conclusion might be applied for lower temperatures, at which it is expected that the purely classical treatment loses its validity. This can be easily shown, when comparing both the spectral moments and the spectral distributions resulting from the two kinds of approach studied here. In order to illustrate the tendency, we decide to discuss the HR effect at a temperature of 95 K—approximately one-third of room temperature.

As far as the spectral profiles are concerned, their shapes for the low-temperature case are presented in Fig. 10, from which one can easily notice that this time the discrepancy between the quantum and purely classical results is really significant, especially for the mid and high frequencies: the difference ranges approximately from $\approx 10\%$ (for the b_1 component) and 5% (b_3) at the line center to 33% and 25%, respectively, at 200 cm^{-1} towards 400% and 500% at above 900 cm^{-1} ! Thus although in the higher temperatures region the classical treatment of the spectra can be accepted in many applications, for lower temperatures it seems to be inevitable to employ the fully quantum theory such as the one mentioned earlier in this paper.

Finally, within the framework of the project we have calculated, both quantum mechanically as well as classically, the integrated intensities (the zeroth moments, in other words) of the obtained b_1 and b_3 parts of the HR profiles. Two independent methods of computing have been used. First, we have estimated the quantities by means of the formulas involving the pair-correlation function approach [Eqs. (25) and (32)], and second, a simple procedure has been applied in order to integrate the numerical spectra over frequencies; the results are presented in Tables II and III. From them it is clearly visible that the agreement between these two methods of calculations is quite satisfactory: the discrepancy is of the order of a fraction of 1%. Conversely, when the quantum and classical moments for the same collisional mechanisms are compared, the difference between them is more pronounced—slightly less evident at 295 K and, obviously—definitely larger at 95 K, which no doubt can be accounted for by the non-negligible role played by the quantum effects in the supermolecules studied. All in all, not only can these results be the reliable check of the validity of our calculations, but also they provide an additional evidence of the important role played by the quantum corrections in the computing procedure, even though it should be admitted that the zeroth moment mainly reflects the properties of a rather limited scope of the spectra, approximately up to about 250 cm^{-1} , at which the limit the integrated intensities achieve their “saturation point.”

To sum up, in this study we present the results of our recent research into the nonlinear properties of the He-Ne system of two-atom colliding supermolecules. New datasets comprising collision induced components of the hyperpolarizability tensor \mathbf{b} obtained by means of the *ab initio* methods of quantum chemistry are given. Their dependence on the interatomic separation is also provided including the case of extremely short distances. The hyperpolarizabilities are next used to compute the hyper-Rayleigh collisional spectral profiles and related quantities characterized the light scattered on a mixture of He and Ne atoms. Both the outline of quantum and classical theory of such spectra and the numerical results are given. Unlike in our previous works the supermolecules analyzed in this paper are expected to exhibit more conspicuously their quantum nature. The results obtained support this thesis, especially for the systems in lower temperatures and at the far wings of the profiles. We also investigate the influence of the particular R range sections of the $b_k(R)$ dependence on the shape and intensities

of the spectral contributions associated with the two possible components of the \mathbf{b} tensor, finding out that their short-range behavior should substantially reflect in characteristic features of the spectral bands. The crucial importance of the b_3 part for the high-frequency spectrum and the depolarization ratio is also emphasized. We believe that in view of the rapid development of very subtle experimental techniques the conclusions presented here seem to serve soon as a useful

tool in future interpretations of the hyper-Rayleigh spectra measured.

ACKNOWLEDGMENTS

This work has been supported in part by Grant No. 1 P03B 082 30 of the Polish Ministry of Education and Sciences. The paper is dedicated to Yves Le Duff on his retirement from the Université d'Angers.

-
- [1] R. W. Terhune, P. D. Maker, and C. M. Savage, *Phys. Rev. Lett.* **14**, 681 (1965).
- [2] S. Kielich, *Bull. Acad. Pol. Sci., Ser. Sci., Math., Astron. Phys.* **12**, 53 (1964).
- [3] S. Kielich, *Acta Phys. Pol.* **24**, 135 (1964).
- [4] Y. Y. Li, *Acta Phys. Sin.* **20**, 164 (1964).
- [5] S. J. Cyvin, J. E. Rauch, and J. C. Decius, *J. Chem. Phys.* **43**, 4083 (1965).
- [6] R. Bersohn, Y. H. Pao, and H. L. Frisch, *J. Chem. Phys.* **45**, 3184 (1966).
- [7] P. D. Maker, *Phys. Rev. A* **1**, 923 (1970).
- [8] K. Clays and A. Persoons, *Phys. Rev. Lett.* **66**, 2980 (1991).
- [9] K. Clays, A. Persoons, and L. DeMayer, in *Modern Nonlinear Optics*, Advances in Chemical Physics Vol. 85 (3), edited by M. Evans and S. Kielich (Wiley, New York, 1993), p. 455.
- [10] D. P. Shelton and J. E. Rice, *Chem. Rev. (Washington, D.C.)* **94**, 3 (1994).
- [11] J. Zyss and I. Ledoux, *Chem. Rev. (Washington, D.C.)* **94**, 77 (1994).
- [12] G. J. T. Heesink, A. G. T. Ruiter, N. F. vanHulst, and B. Bolger, *Phys. Rev. Lett.* **71**, 999 (1993).
- [13] X. Li, K. L. C. Hunt, J. Pipin, and D. M. Bishop, *J. Chem. Phys.* **105**, 10954 (1996).
- [14] *Phenomena Induced by Intermolecular Interactions*, NATO Advanced Studies Institute, Series B: Physics, edited by G. Birnbaum (Plenum, New York, 1985), Vol. 127.
- [15] *Collision- and Interaction-Induced Spectroscopy*, NATO Advanced Studies Institute, Series C: Mathematical and Physical Sciences, edited by G. C. Tabisz and M. N. Neuman (Kluwer Academic Publishers, Dordrecht, 1995), Vol. 452.
- [16] T. Bancewicz, Y. Le Duff, and J. L. Godet, in *Modern Nonlinear Optics*, Part 1, Second Edition, Advances in Chemical Physics Vol. 119, edited by M. Evans (Wiley, New York, 2001), pp. 267–307.
- [17] P. Kaatz and D. P. Shelton, *Mol. Phys.* **88**, 683 (1996).
- [18] R. D. Pyatt and D. P. Shelton, *J. Chem. Phys.* **114**, 9938 (2001).
- [19] P. Kaatz, E. A. Donley, and D. P. Shelton, *J. Chem. Phys.* **108**, 849 (1998).
- [20] T. Bancewicz, J.-L. Godet, and G. Maroulis, *J. Chem. Phys.* **115**, 8547 (2001).
- [21] T. Bancewicz, V. Teboul, and Y. Le Duff, *Mol. Phys.* **81**, 1353 (1994).
- [22] V. Teboul, Y. Le Duff, and T. Bancewicz, *J. Chem. Phys.* **103**, 1384 (1995).
- [23] A. Elliasmine, J.-L. Godet, Y. Le Duff, and T. Bancewicz, *Mol. Phys.* **90**, 147 (1997).
- [24] A. Elliasmine, J.-L. Godet, Y. Le Duff, and T. Bancewicz, *Phys. Rev. A* **55**, 4230 (1997).
- [25] T. Bancewicz, *J. Chem. Phys.* **111**, 7440 (1999).
- [26] A. D. Buckingham, *Adv. Chem. Phys.* **12**, 107 (1967).
- [27] T. Bancewicz, A. Elliasmine, J.-L. Godet, and Y. Le Duff, *J. Chem. Phys.* **108**, 8084 (1998).
- [28] J.-L. Godet, A. Elliasmine, Y. Le Duff, and T. Bancewicz, *J. Chem. Phys.* **110**, 11303 (1999).
- [29] J.-L. Godet, F. Rachet, Y. Le Duff, K. Nowicka, and T. Bancewicz, *J. Chem. Phys.* **116**, 5337 (2002).
- [30] K. Nowicka, T. Bancewicz, J.-L. Godet, and Y. Le Duff, *Mol. Phys.* **101**, 389 (2003).
- [31] T. Bancewicz, K. Nowicka, J.-L. Godet, and Y. Le Duff, *Phys. Rev. A* **69**, 062704 (2004).
- [32] W. Głaz and T. Bancewicz, *J. Chem. Phys.* **118**, 6264 (2003).
- [33] G. Maroulis and A. Haskopoulos, *Chem. Phys. Lett.* **358**, 64 (2002).
- [34] W. Głaz, T. Bancewicz, and J.-L. Godet, *J. Chem. Phys.* **122**, 224323 (2005).
- [35] A. Haskopoulos, D. Xenides, and G. Maroulis, *Chem. Phys.* **309**, 271 (2005).
- [36] G. Maroulis, *J. Phys. Chem. A* **104**, 4772 (2000).
- [37] R. G. Gordon, *Adv. Magn. Reson.* **3**, 1 (1968).
- [38] L. Frommhold, *Adv. Chem. Phys.* **46**, 1 (1981).
- [39] L. Frommhold, *Collision-induced Absorption in Gases* (Cambridge University Press, Dordrecht, 1993).
- [40] G. Placzek and E. Teller, *Z. Phys.* **89**, 209 (1933).
- [41] N. Meinander, *J. Chem. Phys.* **99**, 8654 (1993).
- [42] J. López Cacheiro, B. Fernández, D. Marchesan, S. Coriani, C. Hättig, and A. Rizzo, *Mol. Phys.* **102**, 101 (2004).
- [43] H. Posch, *Mol. Phys.* **46**, 1213 (1982).
- [44] W. Głaz, J. Yang, J. D. Poll, and C. G. Gray, *Chem. Phys. Lett.* **218**, 183 (1994).
- [45] W. Głaz and G. C. Tabisz, *Can. J. Phys.* **79**, 801 (2001).
- [46] H. D. Cohen and C. C. J. Roothaan, *J. Chem. Phys.* **43S**, 35 (1965).
- [47] S. Boys and F. Bernardi, *Mol. Phys.* **19**, 55 (1970).
- [48] T. Helgaker, P. Jørgensen, and J. Olsen, *Molecular Electronic Structure Theory* (Wiley, Chichester, 2000).
- [49] J. Stiehler and J. Hinze, *J. Phys. B* **28**, 4055 (1995).
- [50] M. J. Frisch *et al.*, GAUSSIAN 98, Revision A.7, Gaussian, Inc., Pittsburgh, PA, 1988.
- [51] G. Maroulis and A. Haskopoulos (unpublished).
- [52] P. Karamanis and G. Maroulis, *Comp. Lett.* 1574-0404 **1**, 117 (2005).

- [53] W. H. Press, S. A. Teukolsky, W. T. Vetterling, and B. P. Flannery, *Numerical Recipes* (Cambridge University Press, Cambridge, England, 1996).
- [54] S. M. Cybulski and R. R. Toczyloski, *J. Chem. Phys.* **111**, 10520 (1999).
- [55] T. J. Giese, V. M. Audete, and D. M. York, *J. Chem. Phys.* **119**, 2618 (2003).
- [56] T. Korona, H. L. Williams, R. Bukowski, B. Jeziorski, and K. Szalewicz, *J. Chem. Phys.* **106**, 5109 (1997).
- [57] R. W. Hamming, *Numerical Methods for Scientists and Engineers* (Mc-Graw-Hill/Dover, New York, 1973).
- [58] L. Landau and E. Lifshitz, *Quantum Mechanics, Nonrelativistic Theory* (Addison-Wesley, Reading, MA, 1958).
- [59] C. G. Gray, *J. Phys. B* **4**, 1661 (1971).
- [60] E. Wigner, *Phys. Rev.* **40**, 749 (1932).
- [61] R. W. Hartye, G. C. Gray, J. D. Poll, and M. S. Miller, *Mol. Phys.* **29**, 825 (1975).
- [62] R. T. Pack, J. J. Valentini, C. H. Becker, R. J. Buss, and Y. T. Lee, *J. Chem. Phys.* **77**, 5475 (1982).
- [63] H. B. Levine, *J. Chem. Phys.* **56**, 2455 (1972).
- [64] G. Maroulis, *J. Mol. Struct.: THEOCHEM* **633**, 177 (2003).
- [65] U. Bafile, R. Magli, F. Barocchi, M. Zoppi, and L. Frommhold, *Mol. Phys.* **49**, 1149 (1983).
- [66] M. Chrysos and S. Dixneuf, *J. Raman Spectrosc.* **36**, 158 (2005).
- [67] N. Meinander, G. C. Tabisz, and M. Zoppi, *J. Chem. Phys.* **84**, 3005 (1986).